Comparative study of the modification of multi-wall carbon nanotubes by gamma irradiation and sonochemically assisted acid etching

Saira Bibi [a,b], Tariq Yasin[b], Mohsan Nawaz[a], Gareth J. Price* [c]

a. Department of Chemistry, Hazara University, Mansehra, Pakistan.
b. Pakistan Institute of Engineering and Applied Sciences, Islamabad, Pakistan
c. Department of Chemistry, University of Bath, Claverton Down, Bath, BA2 7AY, UK

* Corresponding author.

Correspondence regarding the paper (GJP): g.j.price@bath.ac.uk, +44 (0)1225 386504

Abstract

Multi-walled carbon nanotubes (CNTs) have been treated with gamma irradiation in air or by using dilute acids (H_2SO_4/HNO_3) combined with 20 kHz ultrasound to compare their effects. The CNT microstructure has been investigated using transmission electron microscopy which revealed that both methods effectively modified the CNTs to overcome aggregation of the nanotubes, resulting in efficient dispersion in ethanol. The nature of the surface modifications was investigated using Raman and FTIR spectroscopies. The introduction of oxygenated species at the CNT surface was detected. At longer treatment times or high ultrasound intensities, the sonochemically assisted acid treatment showed the highest degree of reaction and functionalisation. Modification of the structure with γ-radiation with doses of 100 kGy or 200 kGy also resulted in a reduction of defects, attributed to an annealing and reorganisation process. The observed effects could be correlated with the time and intensity of the ultrasound used or the dose and dose rate of the γ-radiation. Both methods offer the possibility for processes with lower environmental inpact than those that currently exist. Our results also illustrate the importance of careful control over these experimental parameters if optimum results are to be obtained.

Graphical abstract

A comparison of the effects of ultrasound assisted, dilute-acid etching with γ-irradiation in air on MW-CNTs has been performed

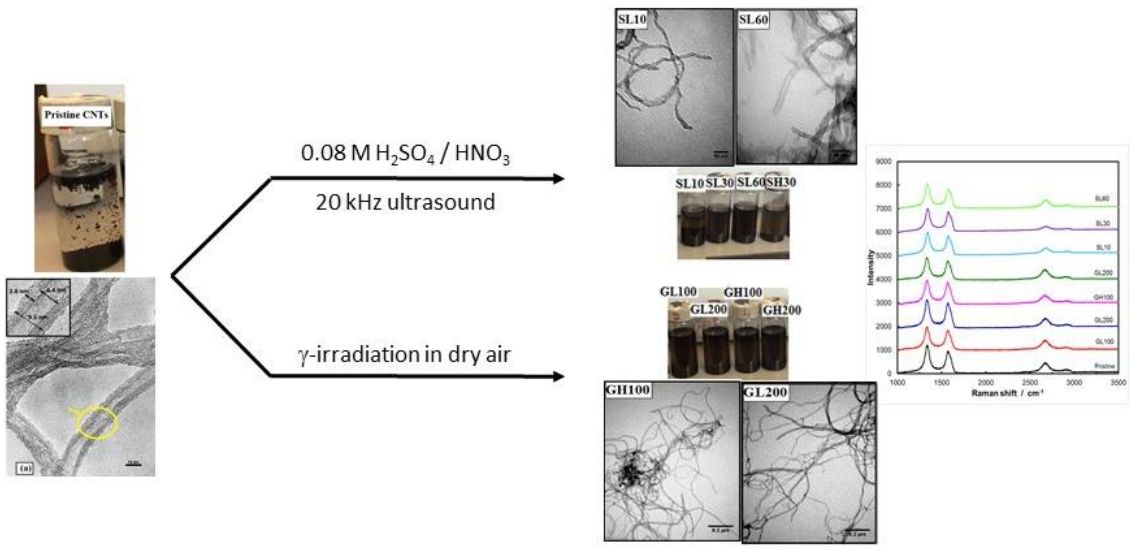

Highlights

- Multi-wall carbon nanotubes have been treated by ultrasound-assisted acid etching and by γ-irradiation
- Both methods change the structure of the CNTs and oxidise their surfaces
- Both methods allow enhanced dispersion of the nanotubes
- Ultrasound allows oxidation at much lower acid concentrations than previously used
- Careful control of experimental conditions is needed if optimum results are to be obtained

1. Introduction

Carbon nanotubes (CNTs) have attracted considerable attention and shown enormous commercial potential in a range of applications [1] due to their unique mechanical, electrical and gas storage properties [2-4]. Their use as reinforcing fillers to increase mechanical strength and elastic moduli as well as other functionality has led to the development of a number of examples of nanocomposite materials containing CNTs [5, 6]. However, strong van der Waals interactions between the nanotubes means that they readily aggregate together and this makes difficult their distribution in a matrix. The hydrophobic and inert nature of the CNTs surface further restricts their application [7, 8]. Functionalization is therefore necessary before use. It has been widely reported that the number of defect sites, their surface properties and the degree of graphitization are important parameters for the characterization of CNTs [9, 10].

Among the methods used to obtain CNTs with controlled properties are coating with surfactants, chemical etching, ultrasonic treatment, mechanical treatment and high energy irradiation [11, 12]. Chemical etching of CNTs is usually carried out by treatment with strong oxidizing agents such as potassium permanganate or highly concentrated solutions of nitric or mixed nitric/sulphuric acids. Using oxidizing acids is more common than other methods due to its easier implementation in laboratory and industrial settings. Detailed observation and analysis by Zhang *et al.* showed that the presence of defects in CNTs plays a crucial role in the oxidation process [13]. Other studies on acid-oxidized CNTs have demonstrated that the degree of functionalization on the surface of the CNTs can be significantly increased when acid treatment is assisted by high power ultrasound [14].

Ultrasound-assisted acid-treatment is therefore potentially an ideal alternative for creating defects and increasing the rate of oxidation reactions while operating under less forcing conditions. The main effects of using ultrasound arise from cavitation; the collapse of micrometer-sized bubbles which are generated during the rarefaction phase when ultrasonic waves pass through a liquid. As the bubbles collapse, strong shock waves and high speed liquid jets are generated [15]. These are strong enough to overcome the van der Waals interactions and disperse the CNT agglomerates. Some C-C bonds within the CNTs may be ruptured, generating active sites at which subsequent chemical reactions can take place [16]. A further advantage is that reactive species such as, in aqueous systems, hydroxyl radicals are produced during cavitation. To illustrate its potential, some years ago Yang *et al.* suggested that ultrasound-assisted functionalization methods might replace conventional acid treatments opening up the possibility of more efficient and cleaner treatment methods [17]. Tian and co-workers also showed that sonication could speed up permanganate oxidation and increase the number of oxygen-containing functional groups at the surface [18]. In further studies, Ng and Manickam demonstrated [19] that the extent of surface reaction could be controlled by varying the sonication time and Huang *et al.* indicated that ultrasound could be used to vary the mean length of the CNTs as well as to prepare the surface for further reaction with a polymer [20]. Other oxidizing agents and organic modifiers have been used in conjunction with ultrasound, albeit at high concentrations and under forcing conditions [21, 22]. Ultrasound has also been applied to CNT modifications in solvents other than water [23, 24].

Gamma-ray irradiation is an alternative method for modifying the physical and chemical properties of CNTs [25, 26]. It allows ready control over the extent of reaction

at low temperatures with lower levels of pollution. Irradiation of CNTs with energetic particles has been demonstrated to create defect sites and molecular junctions [27, 28]. A linear relationship between the amount of γ-irradiation and the introduction of functional groups and defects on CNTs has been reported [28]. Xu *et al.* suggested that the surface functionality and interlayer spacing can be enhanced by γ-ray treatment with consequent changes to the structural order of CNTs and decrease of their inner-wall distance [29]. Danilchenko *et al.* also reported the introduction of defects into CNTs by irradiation [30] while other groups have exploited these effects to functionalize the surfaces of CNTs. [31]. In work directly related to this paper, we established that gamma irradiation under similar conditions to those reported here is a useful pre-treatment for the functionalization of CNTs with silanes [32]. An irradiation dose of 100 kGy was shown to increase graphitization in CNTs while changing the radiation dose or dose rate affected other structural modifications [33].

Despite the large number of publications dealing with modification of CNTs, there have been few systematic studies comparing the various modification methods on identical CNT samples and exploring the implications for particular application such as a nanocomposite filler. In this work, we have performed such a study comparing the effects that the conditions of sonochemical or γ-irradiation have on CNTs and on their use in chitosan nanocomposites. Specifically, this paper describes the modification and characterisation of a batch of multi-walled CNTs (MW-CNTs), allowing us to directly compare and contrast the effect of various experimental parameters. We have compared in detail the effect of ultrasound assisted acid treatment at much lower concentrations than conventionally used. The effect of different reaction conditions (e.g., time and ultrasound intensity) on the CNT structure has been measured along with the effects of

various doses and dose rates of γ-irradiation in dry air. Changes in the surface chemistry and structure have been elucidated using high resolution TEM together with FTIR and Raman spectroscopies.

2. Experimental

2.1. Chemicals and materials

The multi-walled carbon nanotubes used were from the NANOCYL^{TM}(Korea) NC700 series, produced by catalytic carbon vapour deposition. They were in powder form having 90+ % purity, 9.5 nm diameter and 1.5 μm average length. All other chemicals were purchased from Aldrich (UK) and used as received.

2.2. Chemical modification of CNTs with sonochemical treatment

Raw CNTs (20 mg) were suspended by gentle shaking in 36 cm^3 of a mixture of H_2SO_4 and HNO_3 with the concentration of both acids at 0.08 mol dm^{-3} and sonicated with an ultrasonic horn (Sonic Systems L500-2 Processor with a 1 cm dia. horn). The temperature was maintained at 60 °C and sonication conducted for varying times at fixed intensity (measured calorimetrically [34]) or with varying intensity for a fixed time of 30 min. The results below use the following sample codes SL10, SL30, SL60 were used to represent 10, 30, 60 minutes sonication at the lower intensity of 12 W cm^{-2} (L = lower intensity) and SH30 indicates sonication for 30 min at the higher intensity (H = higher intensity) of 18 W cm^{-2} respectively.

2.3. Chemical modification of CNTs with gamma treatment

Irradiation was performed at Pakistan Radiation Services using a ^{60}Co gamma irradiator (Model JS-7900, IR-148, and ATCOP) in dry air at a dose rate of 1.02 kGy h^{-1}, varying the dose from

100 kGy to 200 kGy. Further experiments were carried out using a higher dose rate of 6.18 kGy h^{-1} to deliver the same overall doses. The sample codes here are assigned as GL100 (100 kGy, lower dose rate), GL200 (200 kGy, lower dose rate), GH100 (100 kGy, higher dose rate) and GH200 (200 kGy, higher dose rate).

2.4. Characterization techniques

High-resolution transmission electron microscopy (HR-TEM) was carried out with a JEOL 2010 instrument, having a point resolution of 0.19 nm and operated at an accelerating voltage of 200 kV. Images were recorded photographically. Samples were suspended in ethanol and coated onto a holey carbon grid supported on 300 mesh copper. Other TEM measurements were carried out on a JEOL JEM 1200 EXII instrument operated at an accelerating voltage of 120.0 kV with samples coated on a 200 mesh carbon-coated copper grid. Raman spectra from 300 - to 4000 cm^{-1} were recorded at room temperature under ambient conditions using a Renishaw inVia Raman microscope with 532 nm (Diode pump solid, DPSS) green laser with a charge coupled device detector. FTIR spectra were recorded using a Perkin Elmer Spectrum100 spectrometer at room temperature using a scanning range of 4000 - 450 cm^{-1} and 16 scans at a resolution of 8.0 cm^{-1}.

3. Results and Discussion

3.1. Dispersion of treated CNTs

CNTs have a strong tendency to agglomerate in polar media due to their hydrophobic nature. This is demonstrated in Fig 1 which shows samples of ~100 mg CNTs distributed in ~10 cm^3 ethanol by vigorous shaking and left to settle for 24 hr. The unmodified, pristine CNTs largely agglomerated and settled out of suspension. Visual observation of the suspension suggested that

aggregation started within 1 hr. Conversely, suspension of CNTs treated either sonochemically or by γ-irradiation resulted in much more effective dispersion and some samples appeared visually to maintain high levels of dispersion for up to several weeks. This indicates that some hydrophilic character had been imparted to the CNTs. This dispersion is vital for homogeneous dispersion into, for example, a polymer matrix and hence for optimizing the properties of a nanocomposite material. The quality of the dispersion improved with increasing treatment time, demonstrated by comparing SL10 through to SL60 in Fig. 1.

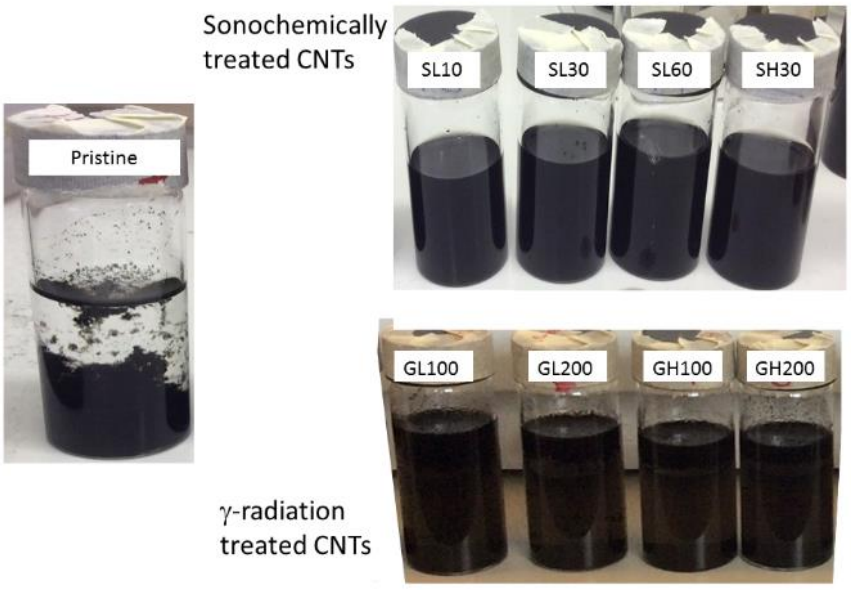

Figure 1. Dispersion of CNTs in ethanol.

The dispersions in ethanol were observed by TEM analysis. Fig. 2 shows TEM images of sonochemically treated CNTs. The micrographs show that the sonochemical treatments led to effective dispersion and separation of individual CNTs; for example, SL30 was well dispersed and well segregated compared with the other samples. Shorter treatment times (SL10) did not fully disperse the nanotubes while after extended times the

nanotubes began to re-aggregate and appeared to be reduced in length (Fig. 3, SL60). The TEM of other samples showed no significant shortening of the nanotubes. This agrees with the work of Huang *et al.* who reported that extended sonication assisted functionalization of CNTs with a polymer resulted in shortening [20]. Our results also demonstrate that the extent of functionalization and dispersion depends on the intensity at which the ultrasonic horn is operated. At higher intensity, (SH30) considerable damage was caused to the CNTs and they formed agglomerates of shorter tubes. It is pertinent to recall here that this work employed much lower concentration of acids than are usually used [11 – 14] and hence represent potentially safer, more environmentally friendly conditions.

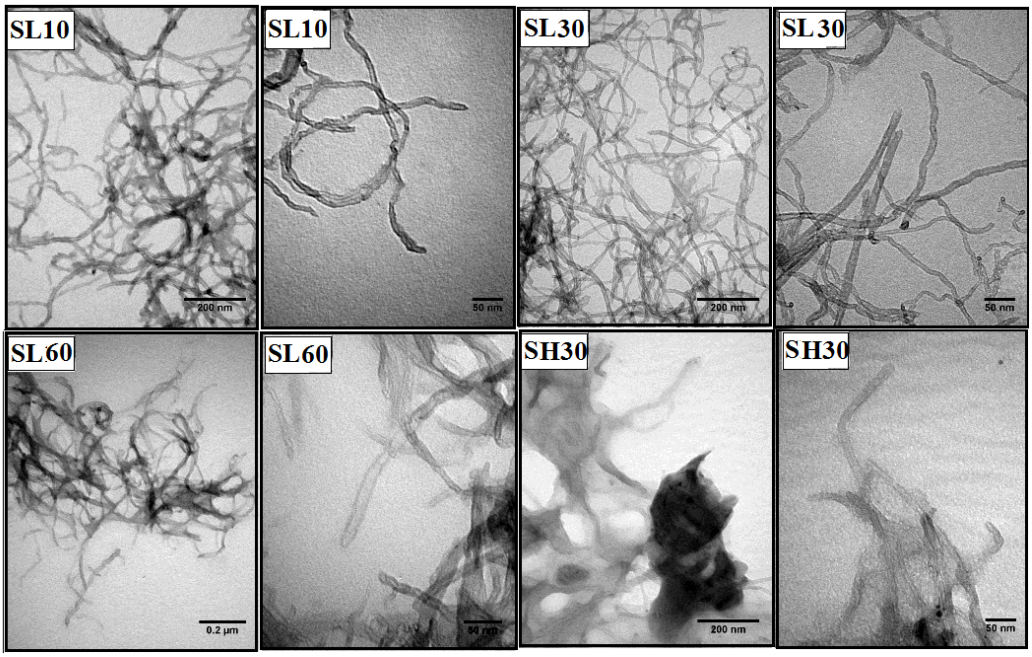

Figure 2. TEM images of sono-treated CNTs. (See text for key to sample codes)

Fig. 3 illustrates TEM images of the γ-treated CNTs dispersed in ethanol. It can be seen that GL100 was well dispersed with no agglomerates; it showed the best dispersion of the four

samples. Treatment at the higher dose rate (GH100, GH200) gave CNTs that retained some agglomerates. This may be due to the lack of mechanical agitation in this method of modification although an alternative explanation would be that the surfaces become highly polar and hence agglomerate through a different mechanism.

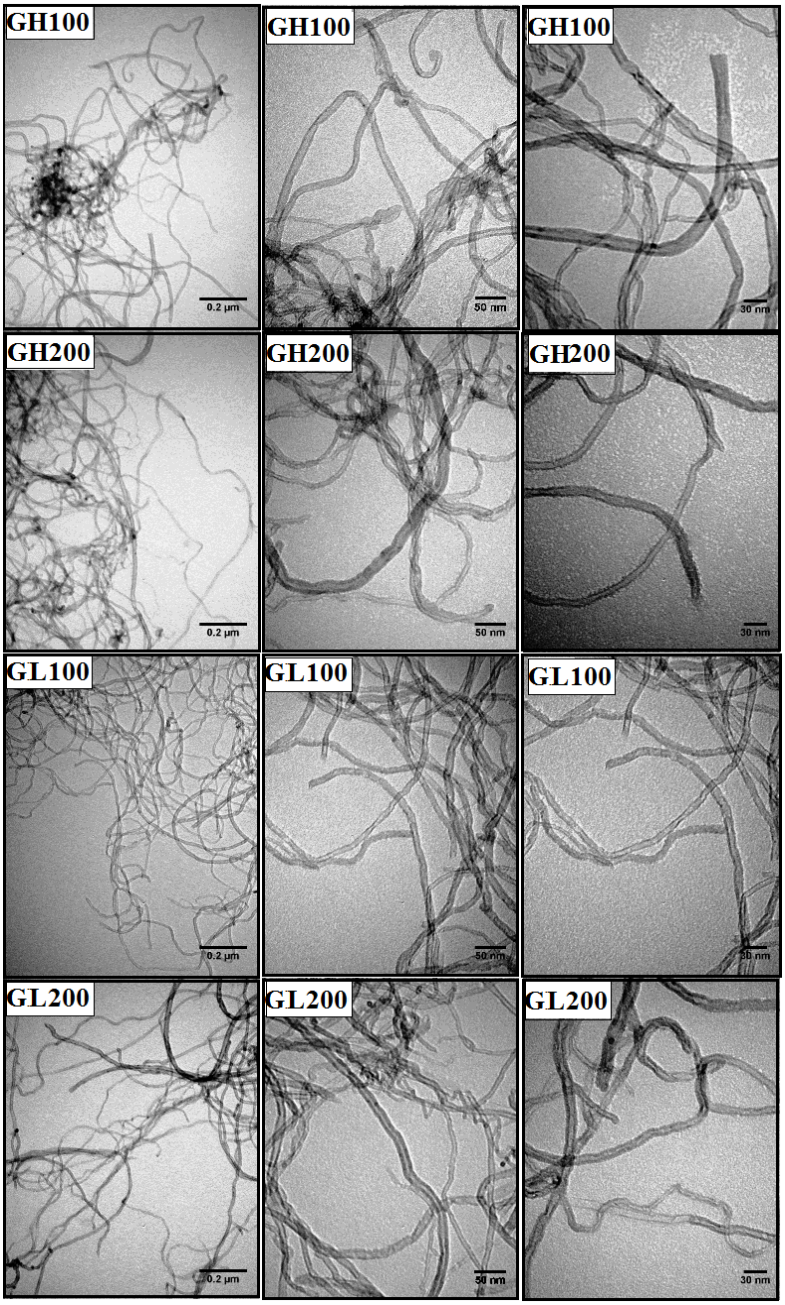

Figure 3. TEM images of gamma-treated CNTs. (See text for key to sample codes)

3.2. Structural evolution during sonochemical treatment

In order to gain further insight into the nature of the surface modifications, higher resolution TEM images were recorded. An example for the pristine CNTs is shown in Fig. 4(a). The bundled structure of adjacent tubes with clear hollow and tubular shapes is clear. The nanotube diameters were ~ 9.5 – 10.6 nm with an average shell thickness of ~2.6 nm while the inner tube diameter was an average of 5.4 nm. The tubes mainly comprised around seven concentric multilayers. In some areas of their surfaces, a coating of amorphous carbon layer can also be observed which had not removed during washing and sample preparation. While it is not possible to compare individual nanotubes, representative samples suggested that in many case, the mean nanotube diameter after 30 min sonochemical treatment (SL30, Fig.4(b)) increased significantly with the wall thickness, ~4 nm, and inner tube diameter also higher than in the pristine CNTs. This expansion of CNTs could have been caused by the formation of amorphous carbon with folding of inner shells by the impact of shock waves and the turbulent motion arising from cavitation.

At longer treatment times (SL60, Fig.4(c)), the structure of CNTs is markedly different. The walls are thinner with a wider, hollow core. Longer treatment, even at the same intensity, causes significant breakage of CNTs and mechanical damage to their surface. Cavitation also produces a large degree of turbulence and the motion and hence high shear forces generated in the fluid could break [18] the CNTs, leading to more open ends. This can be seen when a higher ultrasound intensity was used (SH30, Fig 4(d) inset). Simultaneously with tube breakage, functional groups should build up on the surface of CNTs as a result of enhanced oxidation reactions. The resulting CNT structure

is greatly influenced by increasing the intensity of the ultrasound which would produce higher numbers of cavitation bubbles as well as stronger shear forces and more intense shock waves. Fig. 4(d) also shows there was an increase in surface roughness when the higher intensity was used. This rougher surface can be attributed to the acidic etching of the CNT surface. In general, etching is slow under reflux conditions but is accelerated under sonication. Yang *et al.* also reported [17] that sonication enhanced the rate of oxidation but also caused severe surface damage. In our work, the sonication time was much shorter and did not cause such severe damage (Fig.4(b)). Both the etching and surface damage to the nanotube walls were further accelerated by increasing the intensity of ultrasonic horn.

3.3. Impact of γ-irradiation: morphological effects with varying dose and dose rate

To investigate the effect of the gamma radiation dose rate, pristine CNTs were irradiated in air to 100 kGy at different dose rates (1.06 kGy h^{-1} and 6.0 kGy h^{-1}). The HR-TEM images of CNTs irradiated are shown in Fig. 5. After irradiation up to 100 kGy at the lower dose rate, a dense layer of disordered, carbonaceous material can be seen on the surface of many of the tubes (compare Fig. 5(a), with Fig. 4(a) of pristine CNTs). The walls of the tubes become less well defined and deviate from being straight into a 'zig-zag' pattern. This has previously been observed [35] during γ-irradiation of CNTs and may be the result of irradiation-induced sputtering.

The γ-radiation is sufficiently energetic to break C—C bonds so that rearrangements within the CNTs could take place, potentially generating defects. Some small carbon fragments could also be broken off or ejected and re-condense onto the surface, generating the amorphous

material. In addition the number of layers in the irradiated CNTs is lower, another indication of the sputtering of carbon atoms under the action of γ-radiation. Perhaps more surprisingly, where the higher dose rate was employed, this carbonaceous layer was less dense and more fragmented. The fringes of the walls are clearer although some are distorted and had 'zig zag' fringes (see arrows in Fig 5(b)). When the gamma dose rate was increased to 6.0 kGy/h the diameter of nanotubes were smaller. In addition to direct interaction of the γ radiation with the CNTs, reactive sites produced at the surface could react with atmospheric oxygen to produce functioanlised surfaces. A further reaction path would be via ions produced when air is irradiated.

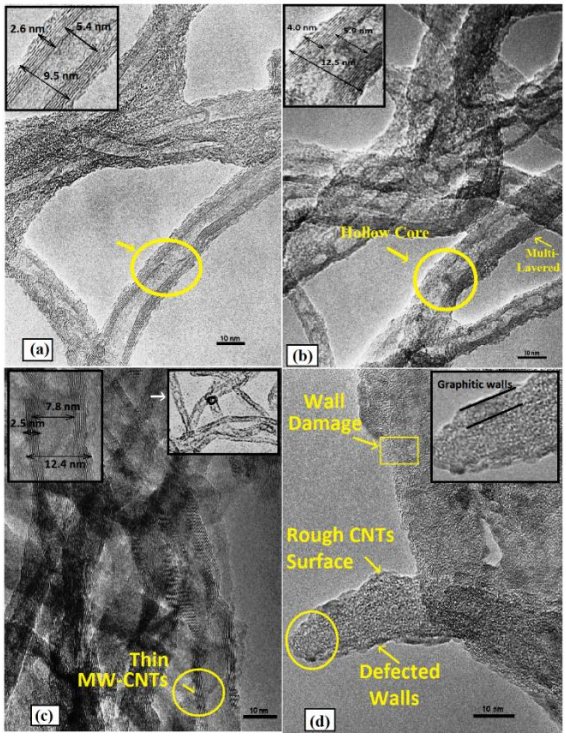

Figure 4. High resolution TEM images for CNTs: (a) pristine; (b) SL30 (30 min at 12 W cm^{-2}); (c) SL60 (60 min at 12 W cm^{-2}); (d) SH30 (30 min at 18 W cm^{-2}). Insets present detailed enlargements of the circled regions

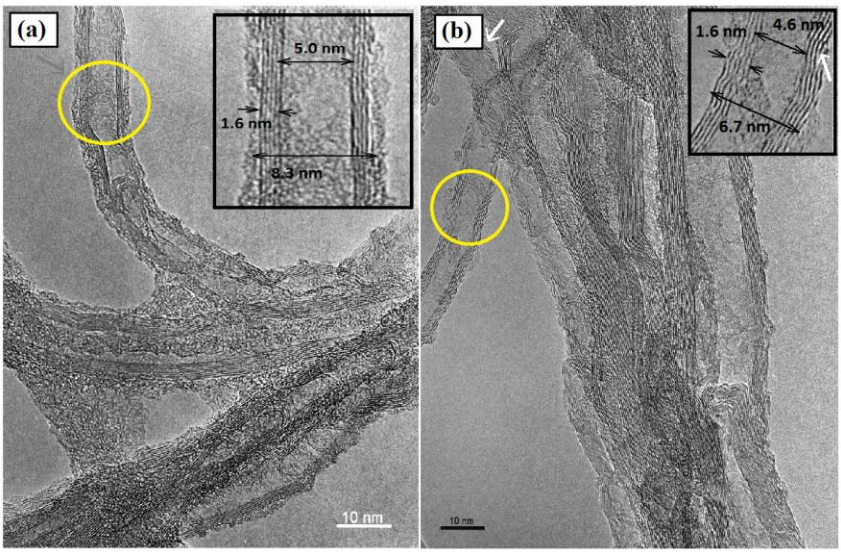

Figure 5. High resolution TEM images of 100 kGy γ-treated CNTs: (a) GL100 (1.06 kGy h^{-1}); (b) GH100 (6.0 kGy h^{-1}). Insets present detailed enlargements of the circled regions.

3.4. Spectroscopic Analysis

Raman spectroscopy can reveal the details of structural changes in CNTs [36]. The spectra of pristine and CNTs modified under different conditions are displayed in Fig. 6. Each of the spectra show the expected three prominent peaks at around 1335 - 1366 cm^{-1}, 1570 - 1581 cm^{-1} and 2667-2682 cm^{-1}. These correspond to the D, G and 2D (or G′) bands respectively. The D-band is characteristic of disordered, defect structures while the G-band is generally assigned to well-ordered sp^2 carbons in a graphite-like structure. The 2D band is an overtone of the D-band. Hence, the ratios of the peak intensities, I_D/I_G, is an indication of the degree of disorder and the number of defects in the materials. The I_D/I_G ratio is sensitive to chemical processing and any physical or chemical changes on the CNTs. The values recorded in this work are shown in Table 1 along with positions of D and G bands and the I_D/I_G , I_{2D}/I_G ratios. Jovanovic *et al.* suggested that the enhancement of the D-band intensity is due to increasing defect density or to decreasing

nanotube length [37]. In the pristine CNTs the, D-band has a maximum at 1338 cm^{-1}. The peak is slightly shifted to higher wavenumber for the sonochemically treated CNTs while it is slightly downshifted for the γ-irradiated samples. Small shifts in the position of the G-band (~ 3-4 cm^{-1}) were also found for the sonochemically treated samples. The observed shifts indicate changes in the chemical environment of bonds at the surface of the CNTs. Stobinski *et al.* [38] suggested on the basis of their FTIR and electron spectroscopy results that the shift may be due to changes in the surface electronic structure by functionalisation with *e.g.* oxygen species. This is supported by our FTIR results discussed below. However in the case of the γ-irradiated samples, the G-band is down shifted by similar amounts. The reasons are less clear here but may be due to the introduction of unsaturation and defects into the CNTs.

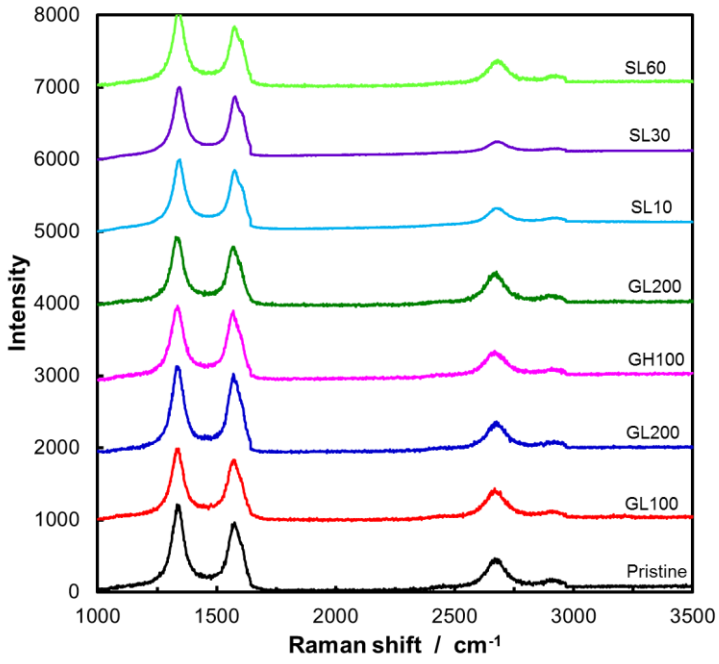

Figure 6. Raman spectra of CNTs. All the spectra have been normalized with respect to the intensity of the G-band. The intensity (arbitrary units) has been shifted up by 1000 for successive spectra.

For the pristine CNTs, the I_D/I_G ratio was 1.556, indicating a large amount of amorphous carbon and/or defects in the starting materials even before treatment. Sonochemical treatment first lowered the ratio although it increased at long sonication time. After 30 minutes ultrasonic treatment in dilute acid, the I_D/I_G ratio decreased by around 5 %. Taking into account the HR-TEM results (Fig 4(b)), this suggests that less amorphous carbon exists on the CNTs and that fewer structural defects result. Chemical reactions such as oxidation may also take place at the defect sites. Extended treatment (SL60) introduces extensive defects and structural disorder into the CNTs, in part due to the large degree of breakage noted above and the increase in open ends as well as extensive surface reaction. The HR-TEM observations suggest that there was less amorphous carbon on the surface so the higher I_D/I_G value is probably due to these additional defects created on the CNT surface. These can result from direct action of the shock waves and shear effects as well as reaction with sonochemically generated radicals and enhanced acid etching.

Fig. 6 and Table 1 also show the corresponding data as a function of gamma irradiation dose and dose rate. Compared with the sonochemical treatment, the I_D/I_G ratios decreased to a greater extent, indicating that the CNTs became somewhat more ordered and lost some of the defects. Moreover, the D-band wavenumber was downshifted by ~2-3 cm^{-1}. There was little difference in band shift between the various irradiation doses. With increasing gamma dose, the I_D/I_G ratio increased slightly although it fell with increasing dose rate. The defects already existing in the CNTs could be annealed to some extent with gamma irradiation. Li *et al.* also reported [35] that the effect of γ-radiation on MW-CNTs increased with dose but passed through a maximum after which the effects were reduced.

Table 1. Raman band positions and ratios for pristine and treated CNTs.

Samples	Wavenumber (cm^{-1})			I_D/I_G	I_{2D}/I_G
	D-band	G-band	2D-band	ratio	ratio
Pristine	1338	1577	2674	1.556	0.658
Sonochemical-treated					
SL10	1343	1579	2677	1.550	0.443
SL30	1343	1581	2684	1.488	0.448
SL60	1341	1580	2680	1.608	0.577
SH30	1342	1580	2680	1.486	0.520
Gamma-treated					
GL100	1336	1573	2671	1.401	0.712
GL200	1337	1575	2675	1.442	0.561
GH100	1335	1571	2669	1.391	0.573
GH200	1335	1573	2670	1.418	0.793

To give further information on the nature of any chemical modification, infra-red spectra were recorded as shown in Figs. 7 and 8. As expected, the spectra of the pristine CNTs indicate no significant level of functionality. Sonochemical treatment results in several peaks appearing in the spectra. After only 10 min reaction, peaks appear at ~2970 cm^{-1}, attributable to C—H stretches, ~1430 cm^{-1} and ~1070 cm^{-1} arising from C—O bonds. At longer treatment times (SL60) or when higher intensities were used (SH30), a broad absorption above 3000 cm^{-1} which arises from O—H was observed together with some indications of carbonyl, C=O, and unsaturated C=C absorptions around 1600-1650 cm^{-1}. Each of these peaks is consistent with the acid etching of the CNT surface. The spectra from the γ-irradiated samples indicated much lower extents of functionalisation and the nature of the modifications were more difficult to discern. However, there are again indications of unsaturated C=C absorptions which are consistent with the Raman and TEM results described above. Further analysis by e.g. zeta potential

measurements or XPS would be needed to unambiguously identify the new functionality that was introduced.

3.5 Further discussion

As noted above, there have been a number of previous studies of sonochemical treatment of CNTs. However, this work has shown that dispersion of the nanotubes together with surface oxidation and modification can be conducted with acids at much lower concentrations than are usually used. For example, Stobinski *et al.* used concentrated (68 %) nitric acid [38] while other workers [39] have used 96% sulfuric acid in conjunction with hydrogen peroxide for up to 5 h. Avilés *et al.* evaluated "mild" oxidation treatments for MW-CNT functionalisation which needed 2 h of sonication with 3 M nitric acid followed by 2 h with hydrogen peroxide or, alternatively, sonication with 8 M mixed nitric/sulfuric acids [40]. Thus, our process, using 100 × more dilute acid, is potentially faster and less environmentally hazardous.

All the work here has been performed using ultrasound with a frequency of 20 kHz. While equipment operating at higher frequencies is available, 20 kHz is most commonly used for sonochemical work and is commercially available for operation on a large scale. However, it is widely recognized that cavitation at 20 kHz maximizes the mechanical effects such as shock waves while higher frequencies tend to produce less motion in the liquid but higher levels of radicals and reactive intermediates. Indeed, Cravotto and co-workers [41] showed that operating in concentrated acids at 300 kHz, oxidation was accelerated while less damage to the CNTs occurred. It would be interesting to use higher frequency ultrasound under the milder conditions employed in this work. An alternative approach could involve a short burst of 20 kHz ultrasound to disentangle the tubes and

provide initial dispersion followed by longer sonication at high frequency to optimize the surface oxidation reactions.

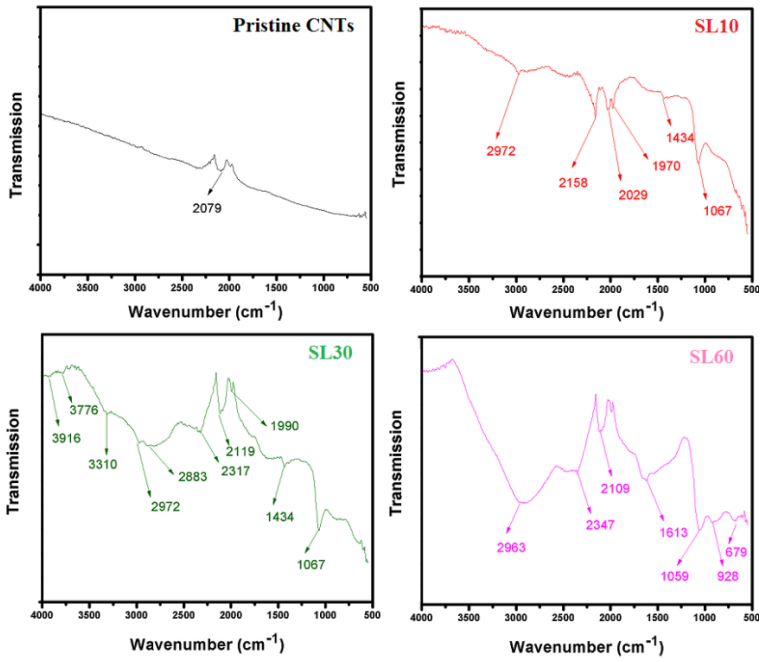

Figure 7. FTIR spectra of sonochemically treated CNTs.

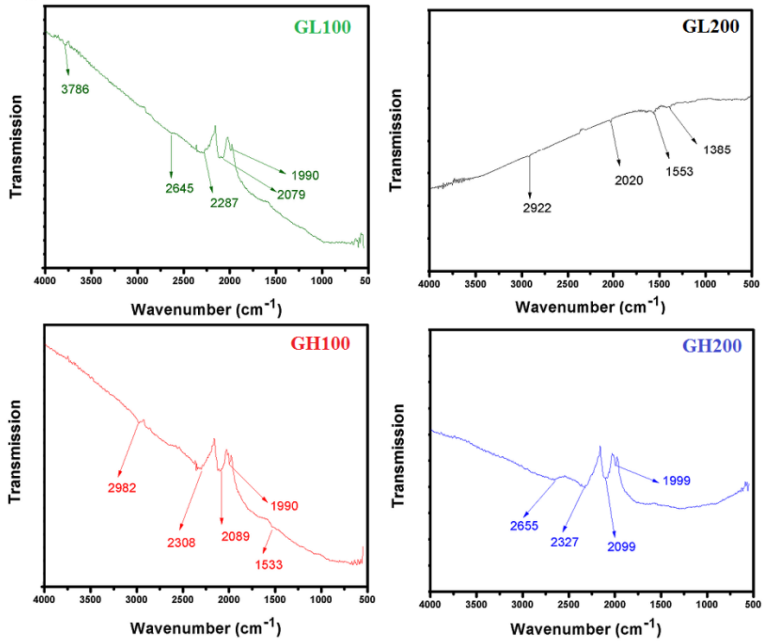

Figure 8. FTIR spectra of γ-irradiated treated CNTs

Some significant differences have been observed between the materials resulting from the sonochemical and the γ-irradiation techniques. There is much more mechanical action in the former and this is reflected in the removal of amorphous material from the CNT surface. Some restructuring and increase of order was seen with the latter method. However, it is apparent that the doses and dose rates used in either case need to be carefully evaluated and controlled if the effects are to be optimised.

The ultimate test of the usefulness of any method is its effect on the final application of the material. The two CNT modification methods outline here have been applied to the manufacture of CNT-containing functional chitosan membranes and the results will be reported in a forthcoming publication.

Conclusions

A systematic comparison of the effect of gamma-irradiation and ultrasound assisted acid oxidation on MW-CNTs has been conducted. Changes in the structure and morphology of the CNTs have been measured. Sonochemical treatment in dilute acid initially leads to a slight reduction in the level of disorder and defects in the structure although these factors can be increased at extended treatment times. The introduction of oxygenated species at the surface was detected. Modification of the structure with γ-radiation also resulted in a reduction of defects, presumably due to an annealing and reorganisation process. The observed effects could be correlated with the time and intensity of the ultrasound used or the dose and dose rate of the γ-radiation. Hence, we suggest that ultrasonic irradiation is the favoured technique solely for introducing oxygen functionalities onto CNTs while γ-radiation is better for their rearrangement and/or restructuring. Given the widespread potential applications of CNT nanocomposite

materials [5, 6, 42], both methods explored here can make a valuable addition to the tools available to the material scientist. However, our results illustrate the importance of careful control over the experimental parameters of either method if optimum results are to be obtained.

Acknowledgements

One of the authors, Saira Bibi, gratefully acknowledges the Higher Education Commission, Pakistan for providing financial funding under IRSIP to visit the University of Bath. We are grateful to Dr Peter Harris at the University of Reading for recording the HR-TEM images, and Dr Ursula Potter at the University of Bath for assistance with the electron microscopy and Raman spectroscopy.

References

1. P.J.F Harris *Carbon Nanotube Science: Synthesis, Properties and Applications* Cambridge University Press (2009)
2. J-Z. Wu, X-Y. Li, Y-R. Zhu, T-F. Yi, J-H. Zhang and Y. Xie, *Ceram. Inter*., 2016, **42**, 9250-9256.
3. M.I. Sajid, U. Jamshaid, T. Jamshaid, N. Zafar, H. Fessi and A. Elaissari, *Int. J. Pharmaceutics*, 2016, **501**, 278-299.
4. M. Boujtita, in *Nanosensors for Chemical and Biological Applications*, Woodhead Publishing, 2014, pp. 3-27.
5. T.E. Chang, A. Kisliuk, S.M. Rhodes, W.J. Brittain and A.P. Sokolov *Polymer* 2006, **47**, 7740–7746
6. J.A. Kim, D.G. Seong, T.J. Kang, J.R. Youn *Carbon* 2006, **44**, 1898–1905
7. Y. Wang, J. Wu and F. Wei, *Carbon*, 2003, **41**, 2939-2948.
8. H. Hiura, T. Ebbesen, J. Fujita, K. Tanigaki and T. Takada, *Nature*, 1994, **367,** 148-151.

9. J.A. Robinson, E.S. Snow, S.C. Badescu, T.L. Reinecke and F.K. Perkins, *Nano Letters*, 2006, **6**, 1747-1751.

10. S.L. Mielke, D. Troya, S. Zhang, J-L. Li, S. Xiao, R. Car, R.S. Ruoff, G.C. Schatz and T. Belytschko, *Chem. Phys. Lett.*, 2004, **390**, 413-420.

11. S. Goyanes, G. Rubiolo, A. Salazar, A. Jimeno, M. Corcuera and I. Mondragon, *Diamond and related materials*, 2007, **16**, 412-417.

12. Y. Yan, J. Miao, Z. Yang, F.X. Xiao, H.B. Yang, B. Liu and Y. Yang *Chem. Soc. Rev.* 2015, **44**, 3295-3346

13. J. Zhang, H. Zou, Q. Qing, Y. Yang, Q. Li, Z. Liu, X. Guo and Z. Du, *J. Phys. Chem. B*, 2003, **107**, 3712-3718.

14. S.E. Skrabalak, *Phys. Chem. Chem. Phys.*, 2009, **11,** 4930

15. K.S. Suslick and G.J. Price, *Ann. Rev. Mater. Sci.* 1999, **29**, 295-326.

16. S. Liang, G. Li and R. Tian, *J. Mater. Sci.* 2016, **51**, 3513-3524.

17. C. Yang, X. Hu, D. Wang, C. Dai, L. Zhang, H. Jin and S. Agathopoulos, *J. Power Sources*, 2006, **160**, 187-193.

18. R. Tian, S. Liang, G. Li, Y. Zhang, L. Shi *Chem. Phys. Lett.* 2016, **650,** 11–15

19. C.M. Ng, S. Manickam *Chem. Phys. Lett.* 2013, **557**, 97–101

20. W. Huang, Y. Lin, S. Taylor, J. Gaillard, A.M. Rao and Y-P. Sun, *Nano Letters* 2002, **2**, 231-234.

21. C.J. Cabello Alvarado, A. Saenz Galindo, C. Perez Berumen, L. Lopez Lopez, C. Avila Orta, J. Valdes Garza, L. Moran Donias *Afinidad* 2014, **71**, 139

22. M. Omastova, M. Micusik, P. Fedorko, J. Pionteck, J. Kovarova, J. Chehimi, M. Mohamed *Surf. Interfac. Anal.* 2014, **46** 940-944

23. Q. Cheng, S. Debnath, E. Gregan, H.J. Byrne *J. Phys. Chem. C.* 2014, **114** 8821-8827

24. M.W. Forney, J.C. Poler *J. Amer. Chem. Soc.* 2010, **132** 791-797

25. B. Safibonab, A. Reyhani, A. Nozad Golikand, S.Z. Mortazavi, S. Mirershadi, M. Ghoranneviss A*pplied Surface Science* 2011, **258**, 766-773

26. V. Skakalova, U. Dettlaff-Weglikowska and S. Roth, *Diamond and Related Materials*, 2004, **13**, 296-298.

27. F. Banhart, *Rep. Prog. in Physics*, 1999, **62**, 1181.

28. J. Guo, Y. Li, S. Wu and W. Li, *Nanotechnology*, 2005, **16**, 2385.

29. Z. Xu, L. Chen, L. Liu, X. Wu and L. Chen, *Carbon*, 2011, **49**, 350-351.

30. B.A. Danilchenko, N.A. Tripachko, I.Y. Uvarova and I.I. Yaskovets, P*hysica Status Solidi (b)*, 2013, **250**, 1488-1491.

31. D. Silambarasan, K. Iyakutti, K. Asokan and V. Vasu, in *SOLID STATE PHYSICS: Proceedings of the 59th DAE Solid State Physics Symposium 2014*, 2015, p. 050088.

32. S. Bibi, T. Yasin, S. Hassan, M. Riaz and M. Nawaz, *Mater. Sci. Eng.: C*, 2015, **46**, 359-365.

33. Z. Xu, L. Chen, B. Zhou, Y. Li, B. Li, J. Niu, M. Shan, Q. Guo, Z. Wang and X. Qian, *RSC Advances*, 2013, **3**, 10579-10597.

34. S Koda, T Kimura, T Kondo, H Mitome, *Ultrason. Sonochem.*, 2003, **10** 149-156

35. B. Li, Y. Feng, K. Ding, G. Qian, X. Zhang, J. Zhang *Carbon* 2013, **60**, 186–192

36. A. Jorio, M.S. Dresselhaus, R. Saito, G. Dresselhaus *Raman Spectroscopy in Graphene Related Systems* Wiley-VCH, Weinheim, Germany, 2011.

37. S.P. Jovanović, Z.M. Marković, D.K.N. Kleut, M.D. Dramićanin, I.D. Holclajtner-Antunović, M.S. Milosavljević, V. La Parola, Z. Syrgiannis and B.M. Todorović, *J. Phys. Chem. C*, 2014, **118**, 16147-16155.

38. L. Stobinski, B. Lesiak, L. Kövér, J. Tóth, S. Biniak, G. Trykowski, J. Judek, *J. Alloys Compounds*, 2010, 501, 77-84.

39. V. Datsyuka, M. Kalyvaa, K. Papagelisb, J. Partheniosa, D. Tasisb, A. Siokoua, I. Kallitsisa, C. Galiotisa, *Carbon* 2008, 46, 833 - 840

40. F. Avilés, J.V. Cauich-Rodrıguez, L. Moo-Tah, A. May-Pat, R. Vargas-Coronado *Carbon* 2009, 47, 2970-2975

41. G. Cravotto, D. de Garella, E.C. Gaudino, F. Turci, S. Bertarione, G. Agostini, F. Cesano and D. Scarano *New J. Chem.* 2011, **35**, 915-919

42. G. Li, T. Zhou, S. Lin, S. Shi and Y. Lin J. Dent. Res. 2017, **96(7),** 725-732.